Relationships Between Complex Core Level Spectra and Materials Properties

C. J. NELIN,[1] P. S. BAGUS,[2] E. S. ILTON,[3] S. A. CHAMBERS,[3] H. KUHLENBECK,[4] H.-J. FREUND[4]

[1]*C. J. Nelin Consulting, Austin, TX 78730*

[2]*Department of Chemistry, University of North Texas, Denton, TX 76203-5017*

[3]*Pacific Northwest National Laboratory, 902 Battelle Boulevard, P.O. Box 999, Richland, WA 99352*

[4]*Fritz-Haber-Institut der Max-Planck-Gesellschaft, Faradayweg 4-6, D-14195 Berlin, Germany*

Received 21 March 2010; accepted 13 April 2010
Published online 24 August 2010 in Wiley Online Library (wileyonlinelibrary.com).
DOI 10.1002/qua.22807

ABSTRACT: The XPS of many oxides are quite complex and there may be several peaks of significant intensity for each subshell. These peaks arise from many-electron effects, which normally are treated with configuration interaction (CI) wavefunctions where static correlation effects are taken into account. It is common to use semiempirical methods to determine the matrix elements of the CI Hamiltonian and there are few rigorous CI calculations where parameters are not adjusted to fit experiment. In contrast, we present, in the present work, theoretical XPS spectra obtained with rigorous CI wavefunctions for CeO_2 where the XPS are especially complex; several different core levels are studied. This study uses an embedded CeO_8 cluster model to represent bulk CeO_2 and the relativistic CI wavefunctions are determined using four-component spinors from Dirac-Fock calculations. In particular, we examine the importance of interatomic many-body effects where there is a transfer of electrons from occupied oxygen 2p orbitals into empty cation orbitals as it is common to ascribe the complex XPS to this effect. We also contrast the importance of many-body charge-transfer effects for the isoelectronic cations of Ce^{4+} and La^{3+}. The long-range goal of this work is to relate the XPS features to the nature of the chemical bonding in CeO_2 and we describe our progress toward this goal. Int J Quantum Chem 110: 2752–2764, 2010

Key words: XPS; many-body; satellites; atomic effects; cerium oxide

1. Introduction

When electronic relaxation and other final state many-body effects are neglected, the X-ray photoelectron spectra (XPS) for core levels will consist of a single line for each of the atomic subshells; see for example, Ref. [1]. In systems where these many-body effects do not dominate, there is a main XPS peak with satellites of low intensity for each of the subshells [2, 3]. However, due to electronic many-body interactions, the XPS

Correspondence to: C. J. Nelin; e-mail: nelin@austin.rr.com

spectra often have complex fine structure with several peaks of significant intensity for a given subshell. This is especially true for materials with open d or f shells, which are often described as highly correlated materials; these include oxides and other ionic crystals [4–6]. Insight into the origin of the spectral features will contribute significantly to an understanding of the electronic structure of these highly correlated materials. Furthermore, the many-body effects may be of both intra-atomic and interatomic origin [5]. While these many-body effects have been discussed for many years, there is still considerable disagreement about the importance of various mechanisms; see Ref. [5] and references therein. A material with unusually complex XPS spectra is CeO_2 [4, 7], which is of considerable interest for its catalytic properties. It is common to assume that charge transfer (CT) from ligands to the open d or f shells of the metal cation is the many body effect that is most important for understanding these XPS spectra [6–8]. However, as we shall show, this view is incomplete. Most theoretical studies, to present, of the XPS of ionic materials in general [6] and of lanthanides in particular [8], have been based on parameterized Anderson model Hamiltonians. On the basis of this model, the core level XPS features have been assigned to a mixing of Ce $4f^0$ O $2p^6$, Ce $4f^1$ O $2p^5$, and Ce $4f^2$ O $2p^4$ configurations. The Anderson model has been used extensively to interpret the spectra of highly correlated oxides; however, agreement with experiment is obtained by fitting semiempirical parameters to experimental XPS data. Such adjustments may neglect important many-body terms and, hence, give misleading results [4, 9]. In this article, we present the results of rigorous theoretical treatments of important aspects of the XPS spectra of crystalline CeO_2 and $LaAlO_3$. Our conclusions are based on the properties of Dirac-Fock (DF) and configuration interaction (CI) wavefunctions [10] for embedded cluster models of these ionic materials. None of the parameters used in the calculation of the wavefunctions were adjusted to fit experimental data. The XPS relative energies, E_{rel}, and intensities, I_{rel}, are taken directly from the calculations without adjustment. The CI wavefunctions are analyzed to identify the features responsible for the XPS spectra. This analysis includes estimation of the occupation of the nominally empty metal 4f and 5d orbitals as well as determination of the weights of configurations without CT, with single CT, and with double CT. We also decompose the orbital relaxation that acts to screen the core-hole into atomic and extra-atomic contributions. As the nominal oxidation states of the metal cations in these compounds, Ce^{4+} and La^{3+}, are isoelectronic with a $4f^0$ occupation, it is reasonable to expect the XPS for these two compounds to be similar; however, our analysis of the orbital relaxation predicts that the spectra will be quite different.

For the interpretation of XPS spectra, it is important to distinguish between XPS allowed and XPS forbidden configurations. To make this distinction, it is useful to consider a wavefunction for the initial state that is a single configuration. This is an acceptable approximation in many cases, especially for the closed shell initial states considered in the present work, as we do not expect dynamic correlation effects [11, 12] to be as important for closed as for open shell systems. In any case, our objective with this separation is to gain a qualitative understanding of how satellites gain intensity and the approximation of a single configuration wavefunction for the N electron initial state is not likely to be a significant concern. To illustrate the separation into XPS-allowed and -forbidden configurations, we use the example of a Ne atom with configuration $1s^22s^22p^6$. As the transition operator for photoionization is a one-electron operator, there are only three XPS-allowed configurations for the $N - 1$ electron final, ionic states [13, 14], where an electron is removed from one of the three occupied shells. These configurations and the approximate binding energies, BE's, of the ionized electron are: $1s^12s^22p^6$ with a BE(1s) = 870 eV; $1s^22s^12p^6$ with a BE(2s) = 45 eV; and $1s^22s^22p^5$ with a BE(2p) = 20 eV. Here, we have neglected the spin–orbit splitting of the 2p(1/2) and 2p(3/2) levels as for Ne, this spin–orbit splitting is small, i.e., $\sim$800 cm^{-1}; on the other hand, the spin–orbit splitting increases rapidly and for Ar, it is 2 eV or 20 times larger [2]. Thus, for heavier atoms, the spin–orbit splitting into $j = \ell + 1/2$ and $j = \ell - 1/2$ must be taken into account. A schematic of the XPS spectra for these allowed configurations is shown in Figure 1. Indeed, this spectra is reasonably similar to the XPS spectra observed for gas phase Ne [3], even though it does not include the weak "shake" satellites [15]. There are, of course, many other configurations for the $N-1$ electron of Ne^+ that are XPS forbidden. For example, the configuration $1s^22s^22p^43d^1$ is XPS forbidden. However, one of the Russell-Saunders multiplets that can arise for

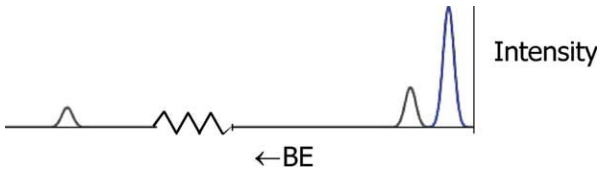

FIGURE 1. Representative XPS Spectra for the Ne atom. [Color figure can be viewed in the online issue, which is available at wileyonlinelibrary.com.]

this configuration is ^{2}S and, hence, this configuration can and does mix with the XPS allowed 2s-hole configuration, $1s^2 2s^1 2p^6$, which is also a ^{2}S multiplet [16]. Thus, the states that would be obtained by a two configuration CI mixing the XPS-allowed 2s-hole configuration and the XPS-forbidden configuration would be one that is dominantly the XPS-allowed 2s-hole configuration and the second, at higher energy, which is dominantly the XPS-forbidden configuration but with a small weight of the XPS-allowed configuration [16]. The second CI state will receive intensity proportional to the weight of the allowed XPS configuration in the CI wavefunction for this state. Thus, it is appropriate to say that the second state, a dominantly XPS-forbidden state, steals intensity from the lower state, which is dominantly the XPS allowed configuration with a small weight of the XPS-forbidden configuration. This interpretation shows us how states dominated by XPS-forbidden configurations are able to gain intensity, possibly considerable intensity, because they contain contributions from the allowed configurations [9, 17]. This analysis is rigorous if one uses the same set of orbitals for the initial, N electron, state, and the final, $N-1$ electron, states. When orbital relaxation to screen the core-hole [18] is taken into account, satellites may also gain intensity because of non-zero overlap integrals between the orbitals of the initial and final states. These shake satellites somewhat blur the concept that we have introduced that dominantly XPS-forbidden states steal intensity from dominantly XPS-allowed states by mixing in CI wavefunctions. However, the concept of stealing intensity by CI mixing is useful for qualitatively understanding the numbers and energy distributions of reasonably intense satellites.

The Ce 3d XPS of CeO_2 shown schematically in Figure 2 shows how, when there are important many-body effects, the simple XPS doublet of a $3d_{5/2}$ peak at lower BE and a $3d_{3/2}$ peak at higher BE with relative intensities of 6:4, corresponding to the occupations of the spin-orbit sub-shells, is lost. In a 40-eV range of energy, there are six XPS peaks with substantial intensity as opposed to the two spin–orbit split peaks expected. In fact, the third peak, at $E_{rel} \sim 20$ eV, has comparable intensity with the first peak at $E_{rel} = 0$; furthermore, the sixth peak at $E_{rel} \sim 40$ eV and the fourth peak at $E_{rel} \sim 25$ eV also have comparable intensities. The common assignment made for these six peaks [7, 8], based on semiempirical Anderson model calculations, is that the first triplet arises from ionization of a $3d_{5/2}$ electron and that the second triplet is from $3d_{3/2}$ ionization. In addition, each of the triplets are assigned as arising, as shown in Figure 2, from mixing of configurations with different degrees of charge transfer. Specifically, these are configurations without CT from O to the empty Ce 4f shell, denoted CT0 for occupations $3d^9 4f^0 O(2p^6)$, configurations with single CT from O to the empty 4f shell, denoted CT1 for occupations $3d^9 4f^1 O(2p^5)$, and configurations with double CT to the empty 4f shell, denoted CT2 for occupations $3d^9 4f^2 O(2p^4)$. Furthermore, the highest BE peaks for each of the triplets, peaks 3 and 6, are assigned as arising from CT0 configurations, while the lower two BE peaks of each triplet are assigned as mixtures of CT1 and CT2 configurations. It is worth noting that these semiempirical calculations are for a generic core-hole; they do not distinguish the properties of different core levels and the spin–orbit splitting is added with an ad hoc parameter. We will demonstrate that our nonempirical calculations indicate that this analysis neglects important intra-atomic many-body effects and the assignment

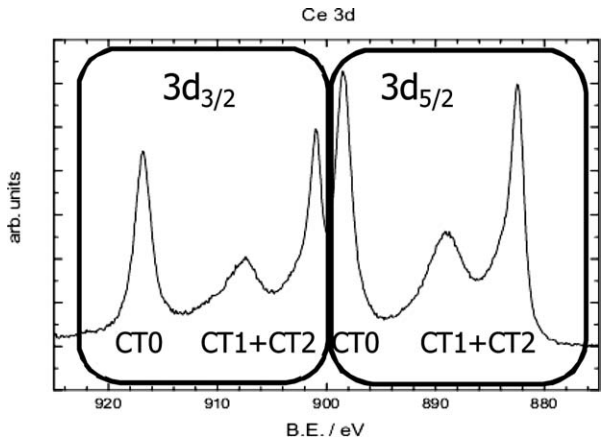

FIGURE 2. CeO_2 3d XPS with semiempirical Anderson Model assignments for the charge transfer origin of satellites.

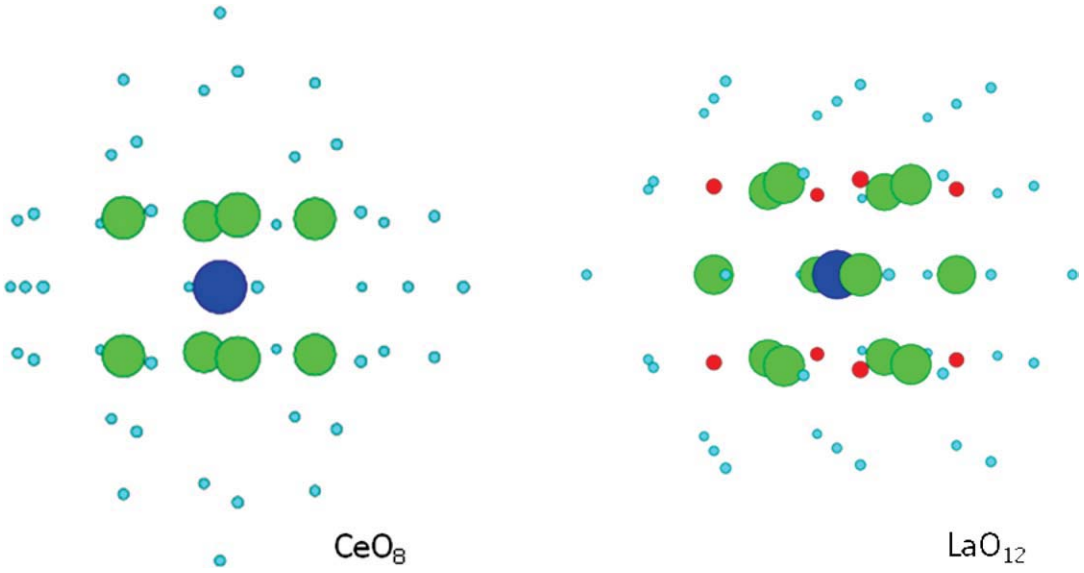

FIGURE 3. Embedded CeO_8 cluster to model CeO_2 and embedded LaO_{12} cluster to model $LaAlO_3$. The atoms explicitly included are shown with larger spheres while the embedding point charges are shown with smaller spheres. [Color figure can be viewed in the online issue, which is available at wileyonlinelibrary.com.]

of the peaks to CT0, CT1, and CT2 configurations is not correct.

In the next section, Theoretical Models, we discuss the models used to determine the wavefunctions for the initial and final, ionized states and the types of many body effects that are included in the CI wavefunctions. We also describe the sudden approximation [18, 19] (SA) model that we use to determine the relative intensities of the different XPS peaks. Finally, we comment on computational bottlenecks for these calculations. In, Results and Discussion, we present results for the 4s and 3d XPS of CeO_2. We also give rigorous definitions for the atomic and extra-atomic relaxation energies, E_R, and contrast the extra-atomic E_R for CeO_2 with that for $LaAlO_3$ leading to a prediction of major differences for the XPS of these two materials. In particular, we argue that these differences arise from the different character of the metal–O covalent interaction between CeO_2 and $LaAlO_3$. Finally, we summarize our conclusions and project directions for future research for the XPS of these and other lanthanide and actinide materials.

2. Theoretical Models

Figure 3 illustrates the embedded CeO_8 and LaO_{12} clusters used as models for the ionic crystals. The central metal cation and its nearest neighbor O anions are treated explicitly and point charges with the values of the nominal ionicities of the anions and cations are placed at the first few shells of next-nearest neighbors of the central cation. The total number of electrons used for the clusters is also chosen based on these nominal ionicities. We have experimented with different sets of point charges and found that the results for the XPS E_{rel} and I_{rel} do not change significantly. For these clusters, we have used a modified version of the DIRAC program system [20] for relativistic wavefunctions (WFs). We have obtained optimized four-component spinors for the initial, unionized, and the final, ionized, configurations where an electron is removed from one of several different core shells of the metal cation; thus, orbital relaxation in response to the core-hole is taken into account [5]. The WFs for the closed shell initial states are one configuration. For the final states, we include many-body effects with CI WF's. The intra-atomic and interatomic configurations included in the CI WF's are described in detail below. Fully uncontracted basis sets were used where the metal atom basis sets are taken from the compilation of Dyall available at the Dirac web site (http://wiki.chem.vu.nl/dirac/index.php/Dirac_Program); the oxygen basis set is the same as used in previous studies of MnO [5] and UO_2 [21]. The theoretical methodologies used are described in Refs. [5, 21].

Although we place our results in the context of previous semiempirical studies [8], we stress that all the results that we present are based on rigorous WF theory. These results do not contain semiempirical parameters to adjust or modify the directly calculated energies and intensities.

For the interatomic many-body effects, we include configurations where one or two electrons are taken from the dominantly O(2p) spinors and placed into an unoccupied cation spinor, either 4f or 5d; we have denoted these charge transfer configurations as CT1 and CT2, see above. In this context, we point out that semiempirical analyses and calculations for lanthanide oxides [7, 8] have been restricted to CT to the cation 4f orbital and have not included CT to the cation 5d orbital. As we show below, CT to the 5d is important for certain satellites. To reduce the size of the CI WFs, we have excluded CT configurations whose matrix element with the reference, CT0, configurations is zero by symmetry [4]. For the CT1 configurations, we are able to include all symmetry allowed configurations in our CI WFs. However, the number of CT2 configurations is too large if we include all allowed configurations and we have used subsets of the possible CT2 configurations. The choices of these subsets were based on orbital symmetries, orbital energies, and the covalent character of the dominantly O(2p) orbitals. The consequences for the predicted XPS spectra from choosing different orbital subsets for the CT2 configurations has been examined and it has been found that, in some cases, the choices may lead to quantitative differences in our XPS predictions, as discussed later.

For the intra-atomic many-body effects, our choice of configurations is based on redistributions of electrons over nearly degenerate orbitals, usually within the shell that contains the core hole. This treatment of static correlation effects [11, 12] leads to major changes in the energy separation and in the number of intense XPS peaks [9, 17, 22]. Of particular importance for many of the core-holes are distributions for which we have coined the term Frustrated Auger Configurations (FACs) [9]. We explain our logic for this terminology by reference to representative FACs for the 4s and 5s hole configurations of Ce^{4+} in CeO_2 shown in Figure 4. For example, for the Ce 5s-hole, the FAC is a configuration where two 5p electrons are moved, one down in energy to fill the 5s shell and on higher in energy into an orbital in the empty 5d subshell. It is this motion of one electron to a more strongly bound orbital and one to a less strongly bound orbital that is the basis of the analogy to an Auger transition. The term frustrated is used because the electron that moves up in energy is still in a bound orbital, while in an Auger transition, this electron is excited into the continuum. In the classification scheme introduced by Sinanoğlu [23], this would be described as an internal excitation as all electrons remain a shell with the same principle quantum number; see also Ref. [24] for the use of this classification to describe excited states. For the Ce 4s-hole, the FAC shown in Figure 4 involves moving an electron down in energy to fill the 4s subshell and moving an electron up in energy into the empty 4f subshell; this FAC is also an internal excitation. However, FACs are not restricted to internal excitations and can also involve semi-internal excitations; such FACs have been shown to be important for the XPS of transition metal oxides [9, 22].

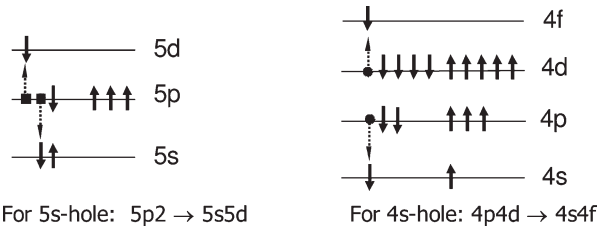

FIGURE 4. Representative frustrated Auger configurations for the 5s and 4s hole states of CeO_2.

For the calculation of the intensities of the XPS transitions, we use the Sudden Approximation, SA, originally formulated by Åberg [18, 19]. In this approximation, the I_{rel} is given as the square of the overlap integral between two $N-1$ electron WFs. The intensity for the ith $N-1$ electron final state, denoted $\Psi_i^F(N-1)$, when an electron is removed from the kth core subshell of the initial state WF denoted $\Psi^I(N)$, is given by:

$$I_{\mathrm{rel}}(i,k) = \left| < a_k \Psi^I(N) | \Psi_i^F(N-1), > \right|^2 \qquad (1)$$

where a_k is an annihilation operator that removes an electron from the kth subshell of $\Psi^I(N)$. The SA also involves summation and averaging over degenerate or nearly degenerate initial and final states, which is not shown in Eq. (1). The SA is exact for very large photon energies but the approximation is valid for photon energies within ~100 eV of the ionization threshold [14, 19]. The SA I_{rel} include the XPS intensities arising from CI

mixing as well as the normally relatively weak shake satellites that arise from orbital relaxation. Because of the final state relaxation, the orbitals of the initial and final states are not orthogonal to each other. In the calculation of the SA overlap matrix element in Eq. (1), we have taken this nonorthogonality fully into account using the method of cofactors [25]. As pointed out in the Introduction, the division into CI and shake satellites is not entirely unique; thus, the use of the SA which gives the intensity for both types of satellites is important. The SA I_{rel} obtained from Eq. (1) are broadened with a Voigt profile [26] for the purposes of direct comparison of our theoretical predictions with experiment. In the present work, as discussed below, we have used only a Gaussian broadening, to minimize the parameters used for the fit.

We close this section by making an estimate of the number of determinants for the CT configurations for the 3d XPS for the CeO_8 cluster model of CeO_2. For this core-hole atomic near degeneracies are not present and we need only take the number of CT determinants into account. For this estimate, we consider only the g and u spinor symmetries and the CI symmetries of Kramers pairs implemented in Dirac (http://wiki.chem.vu.nl/dirac/index.php/Dirac_Program); while use of higher symmetries will reduce the number of configurations, the rapid increase of determinants required for the full treatment of CT effects is clear with this limited symmetry decomposition. There are 10 XPS-allowed determinants corresponding to removal of one of the 10 3d spinors; these 10 determinants have configurations that can be written as $3d^9 4f^0 5d^0 O(2p)^{48}$, where we explicitly show the occupations of the Ce 4f, and 5d, and the O(2p) shells. Taking into account the Kramers pairs, the 10 determinants are treated in two CIs of the order 5. The 48 O(2p) spinors are divided into 24 g and 24 u spinors. For single CT, it is only symmetry allowed to move an $O(2p_u)$ to a 4f spinor or an $O(2p_g)$ spinor to a 5d spinor. With this reduction due to g and u and with the factor of two from the Kramers CI symmetry, the two CIs for the XPS allowed CT0 and the CT1 determinants are of the order 2,885. This is still an easily manageable number of determinants for a CI calculation. However, for the double CT, the numbers of determinants increase dramatically. The symmetry-allowed transfers involve taking $(24) \times (23)/2 = 276$ pairs of $O(2p_g)$ or $O(2p_u)$ and placing them either in two 4f or two 5d spinors or they involve taking 552 pairs of one $O(2p_g)$ and one $O(2p_u)$ spinor and placing them into one of 140 pairs of one 4f and one 5d spinor. Taking the Kramers CI symmetry into account, the number of determinants for each CI is now almost 750,000. While it is not particularly difficult to diagonalize a Hamiltonian matrix of this order for one or a few roots, the XPS studies require that the Hamiltonian be diagonalized for many roots, easily over an energy range of 40 eV, as can be seen from Figure 2. The complete diagonalization of a matrix of order 750,000 will be very demanding of computational resources. Furthermore, the CI for other materials where the cation has nonzero occupation in an open f or d shell is orders of magnitude larger as the spectator electrons in the open shell dramatically increase the number of determinants that must be included so that angular momentum recoupling of the atomic open shells is taken into account [5, 17]. Furthermore, the magnitude of the problem becomes even larger if we wish to include the dynamic electron correlation effects that are necessary if an accuracy of $\sim$0.1–0.25 eV in the XPS E_{rel} is desired. Clearly, the immense CIs needed for the calculation of many-body effects in core-level spectra is the major bottleneck for the accurate theoretical prediction of XPS spectra and methods must be found to reduce the active orbital and configuration spaces. Efforts in this direction are presently in progress.

3. Results and Discussion

We review first our theoretical results for the Ce 4s XPS of CeO_2 [4], where theory and experiment are compared in Figure 5. For the many-body effects, we included the FAC shown in Figure 4, a major subset of the CT1 and CT2 interatomic configurations, as well as cross terms where one electron makes an intra-atomic excitation and one makes an interatomic CT excitation. Further, we checked that the XPS was fairly well converged with respect to the CT2 subset included in our CI WFs [4]. The theoretical I_{rel} were broadened with Gaussians of 3.0 eV full width at half maximum (FWHM) to include the inherent and experimental broadening of the final ionic states. The experimental XPS shown in Figure 5 include the subtraction of a Tougaard-type background [4]. Three of the four theoretical features, labeled A to D in the Figure 5, can be directly correlated to the XPS; the main peak and the two intense satellites

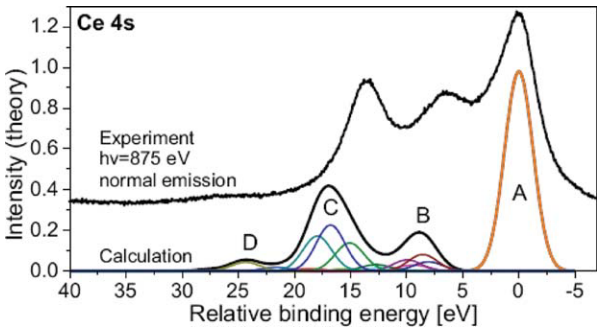

FIGURE 5. Theory and experiment for the 4s XPS of CeO_2. For the theory, intense individual XPS peaks and the envelope of all peaks are shown. The experiment shown in the top curve was measured at the BESSY synchrotron; see Ref. [4]. [Color figure can be viewed in the online issue, which is available at wileyonlinelibrary.com.]

reproduce the main experimental features. The calculated E_{rel} of features B and C are too large by ~3 eV because, with the single orbital set that we have used for our CI WFs, we do not treat the energies of CT configurations as accurately as those without CT [27, 28]. As shown below, Feature A is dominated by CT0 configurations while features B and C are dominated by CT1 configurations and, hence, our computed E_{rel} are somewhat too large. Finally, the weak shake-up satellite at $E_{rel} \sim 24.5$ eV is associated with the intensity in the high BE tail of the XPS. Overall, the agreement of the theory and experiment is quite good, especially considering that we have not included dynamic correlation effects and that we have used a limited set of orbitals preferentially optimized for the CT0 configurations. This agreement provides substantial support for the correctness of our analysis of the nature of the states that contribute to the different XPS structures. Before we turn to this analysis, we note that comparing Figure 2 for the 3d XPS with Figure 5 for the 4s XPS, it is clear that there are important similarities. There are triplets for the 4s and for each of the pairs of 3d peaks. Furthermore, the energy spread of the triplets is similar for the 3d and the 4s XPS and, in both cases, the most intense peaks are the high and low binding energy features. This gives confidence that the conclusions drawn for the electronic structure of the 4s XPS are also relevant for other regions, in particular, the 3d XPS. Later in this section, we will directly test this claim through our preliminary calculations for the 3d XPS.

TABLE I

Analysis of the CT character of selected 4s-hole states. For each state, the E_{rel} and the weights of configurations, Wht(CT0), Wht(CT1), and Wht(CT2), are given.

Feature	E_{rel}(eV)	Wht(CT0)	Wht(CT1)	Wht(CT2)
A	+0.0	0.95	0.01	0.05
B	+8.6	0.01	0.85	0.14
C	+16.8	0.01	0.83	0.16
D	+24.4	0.00	0.66	0.34

We consider the character of the 4s-hole final states with the data shown in Tables I and II for the WFs of representative states in features A through D. In Table I, we give the weights of the configurations without CT, denoted Wht(CT0), with single CT, denoted Wht(CT1), and with double CT, denoted Wht(CT2). These three weights, which include CT to Ce(4f) as well as to Ce(5d), must sum to 1.0. In Table II, we give, for the same representative states shown in Table I, the occupations of important Ce orbitals [$N(i)$] and of the O(2p) orbitals where we give $\Delta N(O_{2p})$, the change from the nominal occupation of 48, to show directly the extent of the charge transfer. These occupations are defined as expectation values of the number operators for the different orbitals. Since there is some covalent mixing of the O(2p) and the Ce 4f and 5d orbitals, the N(4f), N(5d), and $\Delta N(O_{2p})$ values actually represent the occupations of the covalent bonding and

TABLE II

The occupations of the Ce and O 2p orbitals, denoted N(nl) and ΔN(O-2p), in the WF's of the selected states shown in Table I; see text.

Feature	N(4s)	N(4p)	N(4d)	N(4f)	N(5d)	ΔN(O-2p)
A	1.10	5.90	9.90	0.19	0.00	−0.10
B	1.01	5.99	9.99	1.14	0.00	−1.13
C	1.00	6.00	10.00	1.13	0.02	−1.15
D	1.00	6.00	10.00	0.70	0.65	−1.34

antibonding combinations determined in our orbital variations. However, as the same orbitals are used for all states, the trends in occupations are meaningful. The main peak at $E_{rel} = 0$, feature A, is dominated by the contribution of a single final ionic state while there are a few states contributing to each of features B, C, and D. However, the electronic characters of the different states contributing to features B to D are reasonably similar. Thus, it is sufficient to give the data for a single representative state in each of the features. We have chosen the state with the largest SA I_{rel} as the representative state.

A striking feature from Table I is that the main peak, Feature A, arises from a state dominated, with a weight of 95%, by determinants that do not involve charge transfer. The satellite peaks, on the other hand, have very little contribution from configurations without CT. For feature B, Wht(CT0) = 0.012 is the largest weight of configurations without CT for the satellites shown in Table I. Finally, we note that the contribution from double CT, Wht(CT2), to the XPS, while it is not negligible, is not especially large. These three conclusions, obtained from rigorous theory, are in direct contradiction to the results of semiempirical Anderson model calculations [7, 8]. In the Anderson model calculations, the intense feature with the highest E_{rel}, corresponding to our Feature C is found, incorrectly, to be dominated by configurations without CT. On the other hand, single and double CT configurations are claimed to contribute in comparable amounts to the two lower BE peaks, our features A and B. Insight into the character of the 4s-hole states comes from the occupation numbers given in Table II. The Ce 4s, 4p, and 4d occupations change from the ideal values of 1, 6, and 10 because of atomic many body effects; i.e., from the FAC, see Figure 4. For the main peak, feature A, the atomic many body effects involve moving 0.1 4p electrons into the 4s shell and 0.1 4d electrons into the 4f shell. There is a CT of another 0.1 electrons from O 2p into the Ce 4f and there is no CT into Ce 5d. All of the 4s satellites are dominated by CT with very little intra-atomic contributions. See Ref. [4] for further details.

We now present preliminary results for the 3d XPS. In Figure 6, we show the XPS for three different CI treatments; here the calculated I_{rel} were broadened with a Gaussian of 1.6 eV FWHM. The top figure is for only the 10 3d-hole configurations where only spin-orbit splitting is included and there is no CT. There is a small splitting of

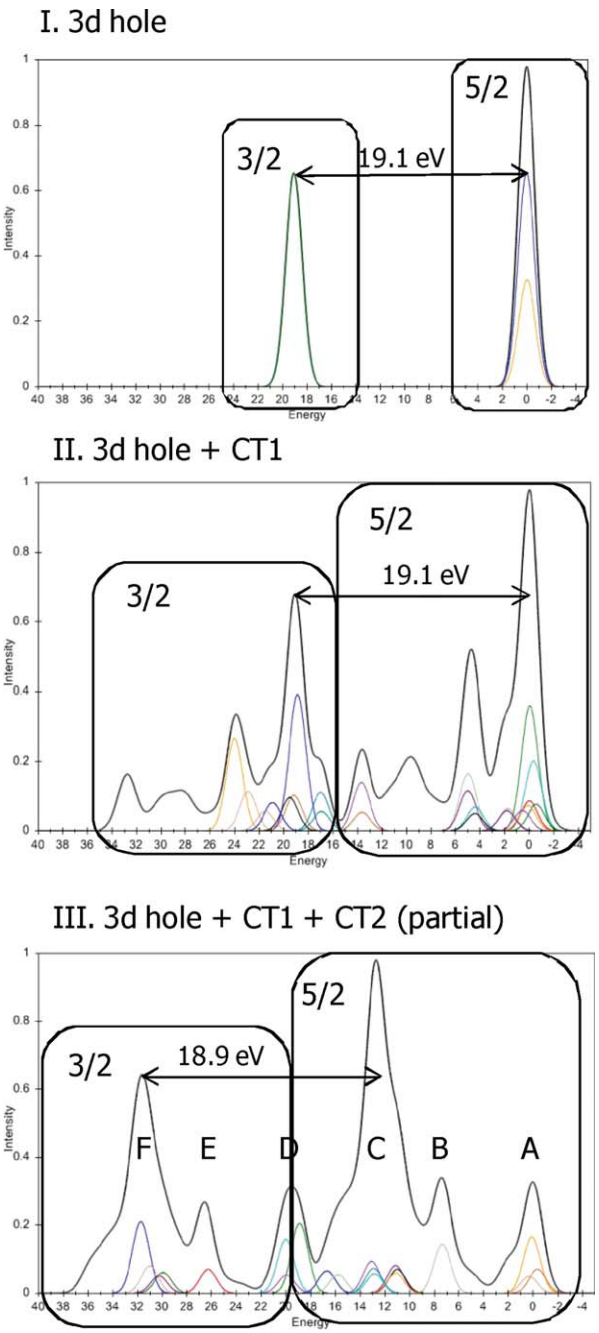

FIGURE 6. Theory for the 3d XPS of CeO_2 showing in I, the hole state with no many-body effects included, in II, the inclusion of single charge transfer configurations, and in III, the inclusion of some double charge transfer configurations. Intense individual XPS peaks as well as the envelope of all contributions are shown. [Color figure can be viewed in the online issue, which is available at wileyonlinelibrary.com.]

TABLE III

Analysis of the CT character of selected 3d-hole states. For each state, the E_{rel} and the weights of configurations, Wht(CT0), Wht(CT1) and Wht(CT2), are given.

Feature	State	E_{rel} (eV)	Wht (CT0)	Wht (CT1)	Wht (CT2)
A	5/2	+0.0	0.40	0.37	0.23
B	5/2	+7.2	0.00	0.37	0.63
C	5/2	+12.0	0.02	0.77	0.22
D	3/2	+18.8	0.51	0.26	0.23
	5/2	+19.8	0.00	0.99	0.01
E	3/2	+26.2	0.01	0.16	0.84
F	3/2	+30.9	0.00	0.95	0.05

the $3d_{5/2}$ peak into a doubly degenerate and a nondegenerate state due to the ligand field; however, the I_{rel} for the 5/2 and 3/2 XPS peaks have the expected 6:4 ratio. The spin–orbit splitting is calculated to be 19.1 eV, about 0.5 eV larger than the splitting in the experimental XPS, see Figure 2. The center curve in Figure 6 is where the full set of single CT determinants has been added. It is clear that this leads to dramatic changes in the XPS and there are now multiple intense peaks for the 5/2 and 3/2 spin–orbit split features. However, the peaks arising from $3d_{5/2}$ and $3d_{3/2}$ ionization continue to be separated by 19.1 eV. The third curve is where a partial set of double CT2 configurations have been added to the CI WFs. There are still further major changes to the predicted XPS and it now shows some resemblance to the observed Ce 3d XPS. Although there are still significant differences, our spectra do contain two sets of triplet peaks as in the experiment. Further, the spin–orbit splitting of the most intense $3d_{5/2}$ and $3d_{3/2}$ peaks is reduced somewhat and is closer to the experimental separation in Figure 2. Furthermore, the separation of the $3d_{5/2}$ and $3d_{3/2}$ features is not as complete as for the two previous curves in the figure. The feature labeled D in the figure has contributions from states where dominant ionization is $3d_{5/2}$ and from others where the dominant ionization is $3d_{3/2}$. While, it is clear that we have not included a sufficiently large set of interatomic many body terms to reach convergence for our description of the Ce 3d XPS, it is valuable to analyze the WF's for our largest CI where both single and double CT configurations have been included in the CI. While we expect that the quantitative features of our results will change when we include more terms in the CI, in a direction that will improve the agreement with experiment, we do not expect the general qualitative characters of the final states to change. Of course, this expectation must be justified with more complete CI WFs.

In Tables III and IV, we present results for representative 3d-hole states that parallel the data presented for the 4s-hole states in Tables I and II. In Table III, we give the weights of the different CT configurations, Wht(CT0), Wht(CT1), and Wht(CT2). In Table IV, we give the orbital occupations for Ce orbitals, N(3d), N(4f), and N(5d), and for the loss of occupation of the O_{2p} orbitals, $\Delta N(O_{2p})$, where these occupations are defined in the same way as for the 4s-hole states. For feature D, we include two representative states, one for a dominantly $3d_{5/2}$-hole and the other for a dominantly $3d_{3/2}$-hole; it is easy to see from the tables that these two states have a different character from each other. For the other features, only a single representative state is given. There are similarities and differences between the characters of the states for the 3d and the 4s XPS.

In Table III, we see that the 5/2 and 3/2 states with the lowest energy have the only large contributions from configurations without CT while the states with higher BE have almost no contribution from configurations without CT. This is similar to what was found for the 4s-hole states and it is in direct contradiction to the results of semiempirical calculations [7, 8]. However, there is a greater mixing of the CT0 with CT1 and CT2 configurations for the lower BE 3d-hole features than for the 4s-hole states. While for the 4s-hole states, only a single state contributed to the lowest BE feature A, see Figure 5, several states contribute to feature A for the 3d XPS. These additional states will allow the intensity from the configurations without CT to

TABLE IV

The occupations of the Ce and O 2p orbitals, denoted N(nl) and ΔN(O-2p), in the WF's of the selected states shown in Table III; see text.

Feature	N(3d)	N(4f)	N(5d)	ΔN(O-2p)
A	9.0	0.82	0.00	−0.82
B	9.0	1.63	0.00	−1.63
C	9.0	1.20	0.01	−1.20
D	9.0	0.70	0.02	−0.70
	9.0	0.21	0.81	−1.01
E	9.0	1.84	0.00	−1.84
F	9.0	1.03	0.01	−1.03

be recovered in the 3d XPS. There is also a much greater importance of CT2 configurations for the 3d-hole states than was found for the 4s-hole states. It is possible that these differences could be due to a different and more complete screening of the deeper 3d core-hole than for the 4s-core hole. Our initial examinations of the O(2p) orbitals for the 3d-hole configuration shows a greater degree of covalent mixing of the O(2p) with the nominally empty Ce 4f and 5d orbitals. However, this apparently greater screening for the Ce 3d-hole needs to be investigated in more detail before firm conclusions can be drawn. The orbital occupations in Table IV show additional evidence for differences between the 3d-hole and 4s-hole final states. As no intra-atomic many body effects were included in the 3d-hole CI wavefunctions, the 3d shell occupation is exactly $N(3d) = 9$. Furthermore, CT to the Ce 5d orbital is significant only for the highest BE $3d_{5/2}$ hole state considered in feature D. It is possible that this is related to the covalent mixing for the screened final state orbitals is between the $O(2p_u)$ spinors with the Ce 4f spinors. Finally, the greater importance of the double CT configurations can be seen from the larger values of $\Delta N(O_{2p})$ for the 3d-hole states than for the 4s-hole states. For example, for the representative state shown for Feature E, $\Delta N(O_{2p})$ is almost -2 consistent with the weight of CT2 configurations, 0.84, in this state, shown in Table III. Overall, the differences between the results for the 4s-hole and 3d-hole states strongly suggest that the concept of a generic core-hole state, used in the semi-empirical calculations [8] may be an oversimplification.

Another way to quantify the screening of hole states is to examine the relaxation energy, E_R, defined rigorously [1] as

$$E_R(k) = E(\text{Koopmans' Theorem}, k) - E(\Delta\text{SCF}, k) \geq 0, \quad (2)$$

where E(Koopmans' Theorem,k) and $E(\Delta$SCF,k) are the energies for the frozen orbital and the fully relaxed variational solutions, respectively, for removal of an electron from the kth subshell. The inequality $E_R \geq 0$ holds rigorously as a consequence of the variational principle and, for closed shell systems, E(Koopmans' Theorem, k) $= -\varepsilon_k$ where ε_k is the Hartree-Fock orbital energy for the kth subshell. It is possible to divide E_R into atomic and extra-atomic contributions [29]. For the specific example of atomic and extra-atomic contributions to E_R for the embedded CeO_8 cluster model of CeO_2, the contributions are defined as follows. The atomic relaxation is the relaxation, from Eq. (2), for ionization of the isolated Ce^{4+} cation, $E_R(Ce^{4+},k)$ and the relaxation, including the extra-atomic screening, is $E_R(CeO_8,k)$. The extra-atomic relaxation is simply the difference of these two relaxation energies, E_R(extra-atomic) $= E_R(CeO_8) - E_R(Ce^{+4})$. The extension of this definition to the La XPS for the LaO_{12} cluster model of $LaAlO_3$ is straightforward. The value of the extra-atomic E_R is that it should provide a guide for the importance of CT satellites in the XPS. If the extra-atomic E_R is small, the chemical interactions, including the covalent bonding, in the final, ionized states is quite similar to the chemical interactions and bonding in the initial, unionized state and it is reasonable that shake satellites [18] and CT satellites will have a weak intensity. On the other hand, large extra-atomic E_R values would be a clear indication of greater screening and greater chemical changes between the initial and final states; hence, one would expect that CT configurations might obtain much more intensity.

TABLE V

The relaxation energy and extra-atomic relaxation energy, in eV, for the 3s-, 4s-, and 5s-hole states for CeO_8 cluster and Ce^{4+} atom are given.

Hole	CeO_8	Ce^{4+}	Extra-atomic
5s	3.1	0.7	2.4
4s	10.1	4.9	5.1
3s	21.4	15.1	6.4

For the Ce 5s, 4s, and 3s hole states of CeO_8, values of the atomic and extra-atomic E_R are given in Table V. The atomic and the cluster E_R increase substantially going to the deeper core levels. This is not surprising since there is a greater contribution from the contractions of the atomic valence and core levels as can be seen from the fact that the atomic E_R for Ce^{4+} increases from 0.7 eV for a 5s-hole to 15 eV for a 3s hole. The increase of the atomic E_R for deeper core-levels is not at all unexpected and has been known for decades [30]. However, the extra-atomic E_R also increases substantially as one goes from shallow to deep core-holes; from Table V, the increase is more than a factor of 2.5 going from a 5s-hole to a 3s-hole configuration. In other words, the deeper core holes cause greater chemical changes and lead to greater screening of the cation core-hole by the ligands. This is fully consistent with

TABLE VI

The relaxation energy and extra-atomic relaxation energy, in eV, for the 4d and 3d hole states for the Ce^{4+} and La^{3+} atoms and CeO_8 and LaO_{12} clusters.

					Extra-atomic	
Hole	Ce^{4+}	La^{3+}	CeO_8	LaO_{12}	Ce	La
4d	4.1	4.3	8.4	6.0	4.3	1.7
3d	16.7	17.0	22.8	18.8	6.1	1.8

our discussion above about the greater importance of CT configurations for the 3d XPS than for the 4s XPS of CeO_2. The greater screening of deeper levels is also found between 3d and 4d ionic configurations.

In Table VI, we compare the E_R for 3d-hole and 4d-hole configurations of CeO_8 and LaO_{12} embedded cluster models of CeO_2 and $LaAlO_3$, respectively. The Ce^{4+} and La^{3+} lanthanide cations in these compounds are isoelectronic, both having empty 4f shells, and one would expect similar chemistry for the two compounds and, hence, similar extra-atomic values for E_R. Indeed since the coordination of the La cation in $LaAlO_3$ is larger than the coordination of the Ce cation in CeO_2, one would expect the extra-atomic E_R to be somewhat larger for the La than for the Ce compound. However, we find exactly the opposite. The atomic E_R are very similar for Ce^{4+} and La^{3+} exactly as one would expect for these isoelectronic cations. Furthermore, the extra-atomic relaxations are larger for the 3d-hole configuration than for the 4d-hole configuration as we found for the 3s and 4s-hole extra-atomic E_R. However, the extra-atomic relaxations for the La d-hole configurations are similar for the 3d and 4d holes and are much smaller than the values for Ce. This is a strong indication of a very different, much reduced, chemistry between La and O than between Ce and O. This reduced chemistry would lead us to expect much less intense XPS satellites due to CT for the La compound than for the Ce compound. We have used the CI WF's that include only spin–orbit splitting to estimate the intensity that would be lost to shake satellites from the *n*d-hole states [18, 31]. For the Ce 4d-holes, 28% of the intensity is lost to satellites while for the 3d-holes, 62% of the intensity is lost to satellites. This is quite consistent with the results that we described earlier in this section for the 4s and 3d satellite structure and it is consistent with our prediction of greater satellite intensity due to CT for deeper core-holes. Again the situation is very different for the SA intensity lost to satellites for the 3d and 4d holes of La in $LaAlO_3$. The intensity lost for 4d-holes to satellites is only 11% about 1/3 of the losses for Ce and the intensity lost for the La 3d-holes is only slightly larger at 15%, which is only 25% of the intensity lost for the Ce 3d-holes. This is consistent with our analysis of the extra-atomic E_R and lends support to our prediction that the La 3d and 4d XPS for $LaAlO_3$ will be much less complex that those observed for CeO_2 [7]. Furthermore, we believe that an important contribution to differences in the final state extra-atomic E_R may arise from differences in the initial state covalent bonding in these two compounds. When this relationship to initial state covalency can be established, it would be an important step forward in our goal of directly linking the complexity of the XPS with the ground state chemistry of the system.

4. Conclusions

One important conclusion from our rigorous calculations using DF and CI WFs is that results obtained from semi-empirical calculations [8] may be in error and must be viewed with caution. This conclusion is especially important because analyses based on these semiempirical calculations are commonly accepted [7] and there should be a greater awareness that the assignments made based on such analyses may not be correct. There are three key differences between the results obtained with our nonempirical WFs and those obtained with the semiempirical Anderson model calculations [8]. First, the energetic order of states where configurations without CT are dominant or important and states where configurations with CT are dominant is reversed. While the semiempirical results of Kotani et al. [8] predict that the states dominated by configurations without CT have the highest BEs within a group of states, we find that they will have the lowest BEs and will often correspond to the main peaks. It is worth noting that similar claims about the energetic order of states, based on considerations for Anderson model Hamiltonians, have been made for ionic transition metal compounds [32, 33]; thus it is possible that these semiempirical

calculations have a systematic bias for the energies of configurations that have CT. Second, we find that atomic many-body effects may need to be taken into account. It is possible to extend the Anderson model Hamiltonian formulation to include atomic many-body effects and this has been done in treatments of the XPS of transition metal oxides [32, 34]. However, atomic many-body effects have not been included in the Anderson model semiempiridal study of CeO_2 [8]. Third, we find differences in the importance of CT configurations for the energetic positions and, especially, for the intensities of satellites depending on the core-hole created. In part, we are able to explain these differences in the XPS satellites in terms of the different extra-atomic screening of the core-hole configurations with this relaxation being smaller for the shallower core-hole configurations and larger for deeper core-hole configurations.

Another important prediction that we make is that the satellite structure will be very different for what one might naively expect to be closely related oxides of Cerium and Lanthanum because of the different final state extra-atomic relaxation in the two oxides. It will be important to understand why these differences exist and to relate them to the differences in the electronic structure of these two materials. We have noted that screening through orbital relaxation blurs the distinction between shake and charge transfer satellites. It will be important to resolve this blurred distinction, especially since we have shown that extra-atomic screening may provide a useful guide to the intensity and complexity of the XPS satellite structure. This distinction does not appear to have been explicitly treated in the extensive literature on the complex XPS spectra of highly correlated oxides and of other ionic materials.

There is considerably more effort required to improve and make more realistic our theoretical treatments of core-level XPS spectra, especially in terms of refining definitions of the active configuration and orbital spaces. However, the results reported here, clearly show that these improvements will enable us to reach the objective of using and interpreting XPS spectra to understand chemical bonding in these highly correlated systems.

ACKNOWLEDGMENTS

We acknowledge support by the Geosciences Research Program, Office of Basic Energy Sciences, U.S. DOE and by the DFG through their SFB 546, "Transition Metal Oxide Aggregates." Computer support from the Pittsburgh Supercomputer center is also acknowledged. A portion of the research was performed in the Environmental Molecular Sciences Laboratory at PNNL.

References

1. Bagus, P. S.; Illas, F.; Pacchioni, G.; Parmigiani, F. J Electron Spectrosc Relat Phenomena 1999, 100, 215.
2. Siegbahn, K., Nordling, C.; Fahlman, A.; Nordberg, R.; Hamrin, K.; Hedman, J.; Johansson, G.; Bergmark, T.; Karlsson, S. E.; Lindgren, I.; Lindberg, B. ESCA-Atomic, Molecular, and Solid State Structure Studied by Means of Electron Spectroscopy. Almqvist and Wiksells: Uppsala, Sweden, 1967.
3. Siegbahn, K., Nordling, C.; Johansson, G.; Hedman, J.; Hedén, P. F.; Hamrin, K.; Gelius, U.; Bergmark, T.; Werme, L. O.; Manne, R.; Baer, Y. ESCA-Applied to Free Molecules. Amsterdam: North Holland, 1969.
4. Bagus, P. S.; Nelin, C. J.; Ilton, E. S.; Baron, M.; Abbott, H.; Primorac, E.; Kuhlenbeck, H.; Shaikhutdinov, S.; Freund, H. J. Chem Phys Lett 2010, 487, 237.
5. Bagus, P. S.; Ilton, E. S. Phys Rev B 2006, 73, 155110.
6. de Groot, F. M. F. J Electron Spectrosc Relat Phenomena 1994, 67, 529.
7. Mullins, D. R.; Overbury, S. H.; Huntley, D. R. Surf Sci 1998, 409, 307.
8. Kotani, A.; Jo, T.; Parlebas, J. C. Adv Phys 1988, 37, 37.
9. Bagus, P. S.; Broer, R.; Ilton, E. S. Chem Phys Lett 2004, 394, 150.
10. Visscher, L., Visser, O.; Aerts, P. J. C.; Merenga, H.; Nieuwpoort, W. C. Comput Phys Commun 1994, 81, 120.
11. Valderrama, E.; Ludena, E. V.; Hinze, J. J Chem Phys 1999, 110, 2343.
12. Cioslowski, J. Phys Rev A 1991, 43, 1223.
13. Bethe, H. A.; Salpeter, E. W. Quantum Mechanics of One- and Two-Electron Atoms. Academic Press: New York, 1957.
14. Bagus, P. S.; Viinikka, E. K. Phys Rev A 1977, 15, 1486.
15. Manne, R.; Aberg, T. Chem Phys Lett 1970, 7, 282.
16. Bagus, P. S.; Broer, R.; Parmigiani, F. Chem Phys Lett 2006, 421, 148.
17. Bagus, P. S.; Broer, R.; de Jong, W. A.; Nieuwpoort, W. C.; Parmigiani, F.; Sangaletti, L. Phys Rev Lett 2000, 84, 2259.
18. Aberg, T. Phys Rev 1967, 156, 35.
19. Sangaletti, L.; Parmigiani, F.; Bagus, P. S. Phys Rev B 2002, 66, 115106.
20. Saue, T.; Bakken, V.; Enevoldsen, T.; Helgaker, T.; Jensen, H. J. A.; Laerdahl, J. K.; Ruud, K.; Thyssen, J.; Visscher, L. Dirac, a relativistic ab initio electronic structure program; Release 3.2, 2000. http://wiki.chem.vu.nl/dirac/index.php/Dirac_Program.

21. Ilton, E. S.; Bagus, P. S. Surf Sci 2008, 602, 1114.
22. Bagus, P. S.; Broer, R.; Ilton, E. S. J Electron Spectrosc Relat Phenomena 2008, 165, 46.
23. Sinanoglu, O. Adv Chem Phys 1969, 14, 237.
24. Nicolaides, C. A. Int J Quantum Chem 2005, 102, 250.
25. Prosser, F.; Hagstrom, S. J Chem Phys 1968, 48, 4807.
26. Gubner, J. A. J Phys A Math Gen 1994, 27, 745.
27. Hozoi, L.; de Vries, A. H.; Broer, R.; de Graaf, C.; Bagus, P. S. Chem Phys 2006, 331, 178.
28. Bagus, P. S.; Broer, R.; de Graaf, C.; Nieuwpoort, W. C. J Electron Spectrosc Relat Phenomena 1999, 99, 303.
29. Egelhoff, W. F. Surf Sci Rep 1987, 6, 253.
30. Bagus, P. S. Phys Rev 1965, 139, A619.
31. Bagus, P. S.; Schrenk, M.; Davis, D. W.; Shirley, D. A. Phys Rev A 1974, 9, 1090.
32. Okada, K.; Kotani, A. J Phys Soc Jpn 1992, 61, 4619.
33. Veal, B. W.; Paulikas, A. P. Phys Rev B 1985, 31, 5399.
34. Sangaletti, L.; Depero, L. E.; Bagus, P. S.; Parmigiani, F. Chem Phys Lett 1995, 245, 463.